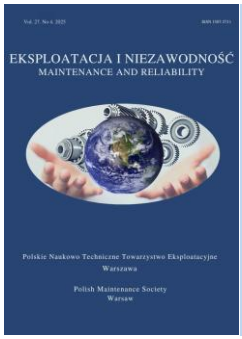

Eksploatacja i Niezawodnosc – Maintenance and Reliability

Volume 27 (2025), Issue 4

journal homepage: http://www.ein.org.pl

Article citation info:
Shi R, Lü Y, Zhang Y, Meng J, Hu R, Remaining Useful Life Estimation with Coupling Dual Random Effects Based on Nonlinear Wiener Process, Eksploatacja i Niezawodnosc – Maintenance and Reliability 2025: 27(4) http://doi.org/10.17531/ein/202908

Remaining Useful Life Estimation with Coupling Dual Random Effects Based on Nonlinear Wiener Process

Indexed by: Web of Science Group

Rui Shi[a,b], Yanjun Lü[a,*], Yongfang Zhang[c], Jiacheng Meng[a], Ruibo Chen[a], RuiYing Hu[a]

[a] School of Mechanical and Precision Instrument Engineering, Xi'an University of Technology, China
[b] Ningxia Vocational Technical College of Industry and Commerce, China
[c] Faculty of Printing, Packaging Engineering and Digital Media Technology, Xi'an University of Technology, China

Highlights

- A coupling dual random effects are considered in the nonlinear WP degradation process.
- An extended EM algorithm is presented to estimate the hidden parameters of the model.
- The method is validated by using the rolling bearings and areo-engines dataset.
- The proposed model and method can effectively estimate RUL of different equipment.

Abstract

The influencing factors of performance degradation play a crucial role in accurately estimating the Remaining Useful Life (RUL) of equipment. Based on a nonlinear Wiener degradation process, a stochastic degradation model with coupled dual random effects is proposed to capture the degradation process of equipment under complex working conditions. The analytical expression of the Probability Density Function (PDF) for the RUL of the model, considering asymmetric distribution of drift and diffusion coefficients, is obtained by applying total probability formula. Based on Bayesian theory and its posterior distribution, an extended Expectation Maximization (EM) algorithm is employed to estimate the hidden and other parameters of the degradation model. Experimental investigations are carried out using the rolling bearing dataset from XJTU-SY and the turbofan aero-engine dataset from NASA. The effectiveness of the proposed model and approach is compared with that of the existing models in previous studies. The results show that the proposed model exhibits high RUL estimation accuracy.

Keywords
remaining useful life, nonlinear Wiener degradation process, dual random effects, expectation maximization algorithm

1. Introduction

Efficient and accurate Prognostics and Health Management (PHM) are essential for enhancing equipment safety, integrity, and reducing maintenance costs[1]. This is particularly crutial for long-life, highly reliable aero-engines and similar products. The Remaining Useful Life (RUL) estimation within PHM holds significant importance[2]. However, estimating RUL for long-life, high-reliability products is challenging due to the scarcity and high cost of historical degradation information. Typically, the performance tends to degrade during operation[3]. Many factors affect performance degradation, including external environmental conditions, internal materials, manufacturing processes, etc. Identifying the specific causes and factors responsible for performance degradation is often difficult. The use of data-driven approaches has become

(*) Corresponding author.
E-mail addresses: R. Shi (ORCID: 0009000338564370) destiny01314@163.com, Y. Lü (ORCID: 0000000239747705) yanjunlu@xaut.edu.cn, Y. Zhang (ORCID: 0000000195097834) zhangyf@xaut.edu.cn, J. Meng 1254459833@qq.com, R. Chen (ORCID: 0009000038341618) 1220211018@stu.xaut.edu.cn, R. Hu 1394775483@qq.com

a promising route for RUL estimation[4-6]. These approaches permit the direct utilization of equipment condition monitoring data or historical data, without relying on physical models of equipment performance degradation. However, achieving higher estimation accuracy demands a substantial amount of data, which may introduce errors when extrapolated over extended intervals.

Currently, RUL is usually estimated based on regression[7, 8], similarity[9], and degradation models[10, 11]. The random coefficient regression model has limitations in accurately capturing the dynamic and time-varying nature of equipment degradation, making it unsuitable for online RUL estimation[12]. Additionally, RUL estimation based on similarity requires multiple historical degradation records of the same equipment type as samples. By integrating multiple factors affecting performance degradation into a comprehensive model, accurate and reliable RUL estimation can be achieved[13]. Degradation models[13-15] considering trajectory, quantity distribution, cumulative damage, and stochastic process have been established. The Wiener Process (WP) model is a commonly used fundamental stochastic process model among the existing performance degradation models[16]. The degradation model of WP can describe both monotonic degradation processes and continuous non-monotonic nonlinear degradation processes with varying tendencies[17]. Recently, many researches have been conducted on understanding nonlinear WP models. For instance, the degradation of the equipment was modeled using a nonlinear drift WP model[18]. Additionally, a novel distributed model fusion method was presented to estimate the RUL with a nonlinear WP[19, 20]. Similarly, an online RUL estimation method based on a generalized nonlinear degradation model with deterministic and stochastic parameters was proposed[21]. To account for the dynamic environmental impacts and loading conditions, a nonlinear WP model with a stochastic time-varying covariate was proposed[22]. These studies have focused on the specific nonlinear degradation models or methods centered around nonlinear WP to address relevant issues. However, in terms of constructing multi-parameter coupling models and handling complex parameter interactions, they lack model adaptability, accuracy and reliability in real applications.

When estimating the RUL of equipment in a nonlinear stochastic degradation process, it's necessary to obtain and solve the analytical expressions of the RUL distribution function corresponding to the failure threshold. Despite the complexity, this approach is effective[23, 24]. Theoretical derivations can yield a general procedure for acquiring these expressions. Usually, the moment when the equipment firstly reaches the failure threshold is referred to as the First Hitting Time (FHT), representing the life of the equipment[25]. The preset failure threshold is generally determined based on engineering experience and technical standards. The degradation process crossing a fixed threshold resembles the standard Brownian Motion (BM) process crossing a time-varying threshold[26]. Corresponding degradation models with failure thresholds are proposed for different equipment clusters[27].To cut calculation costs, fixed thresholds are commonly used for RUL estimation and reliability analysis. It's generally assumed that if the degradation process reaches the threshold at a certain time, the probability of crossing it earlier is negligible. For instance, one RUL estimation method checks if the degradation amount of the equipment exceeds a given threshold limit[28].

The estimation of the parameters in the probability density function (PDF) is essential for RUL estimation. The commonly used parameter estimation methods include moment estimation[29], maximum likelihood estimation[30], least squares estimation[31] and Bayesian estimation[32, 33]. Many scholars have studied alternative parameter estimation methods beyond these established methods[18, 34-36]. The Expectation Maximization (EM) algorithm is commonly used for parameter estimation in probabilistic models with hidden variables, where it iteratively optimizes the model parameters to maximize the likelihood function of the observed data[37, 38]. Although the EM algorithm is sensitive to the initial value, the unknown parameters in the stochastic process model have hidden variables, making the EM algorithm a more suitable choice for parameter estimation.

In summary, through precise parameter settings, this paper considers the coupling relationship between individual and external factors of the nonlinear WP model to capture the degradation process of equipment under complex working conditions. Next, by applying the concept of FHT, through theoretical derivations and mathematical transformations, the

derivation process of the analytical expression of the PDF for the RUL is introduced. Based on Bayesian theory and posterior distribution, an extended EM algorithm is employed to estimate hidden parameters and other key parameters in the model. To validate the accuracy and reliability of the proposed RUL estimation approach, experimental investigations are provided under different working conditions and equipment types. Finally, the conclusions are drawn.

2. Degradation Model with Dual Random Effects

During the manufacturing process, batches of equipment of the same type may show variability due to various factors, including raw material, production processes, etc. These individual differences is typically reflected as drift coefficient in the degradation model. The external random factors can also affect the degradation performance, which can be reflected in the diffusion coefficient. Therefore, individual differences and external factors can be taken into account in performance degradation model is specifically manifested as drift and diffusion coefficients. A nonlinear WP degradation model simultaneously considers the coupling relationship between individual differences and external factors is presented. The initial degradation level is defined as $X(0) = 0$, and the degradation value at time t_k can be denoted by

$$X(t_k) = X(0) + \nu \int_0^{t_k} \Lambda(z, b)\, \mathrm{d}z + \sigma B(t_k) \tag{1}$$

Where ν is the drift coefficient, σ is the diffusion coefficient, $B(t_k)$ is the standard Brownian motion (BM), and $\int_0^{t_k} \Lambda(z, b)\, dz = \mu(t_k; b)$ is the nonlinear function, representing the trend term of the degradation process. Nonlinear functions can take various forms, including polynomials, exponential functions, and power functions[21]. Let $\sigma = 1/\sqrt{\delta}$, and the parameter δ follows a Gamma distribution with shape parameter α and scale parameter β, denoted as $\delta \sim Gamma(\alpha, \beta)$. Under the given parameter δ, the drift coefficient ν follows a normal distribution with mean $\mu_\nu$and variance σ_ν^2, denoted as $\nu|\delta \sim N(\mu_\nu, \sigma_\nu^2)$. Let $\sigma_\nu^2 = \phi/\delta$, where ϕ is the unknown parameter. Because of δ, there is a coupling relationship between drift and diffusion. The precise parameter settings are established through the stochastic distributions and coupling relationships of different parameters. The reason for choosing the random distribution of δ, ν is from Bayesian linear regression for computational convenience[39]. This model is denoted as M1.

To establish the relationship between the performance degradation model and its life expectancy, it is conventionally postulated that the performance degradation process of the equipment adheres to a monotonically increasing tendency. Once the degradation trajectory of the equipment surpasses the preset failure threshold W, the equipment is regarded as being in a failure state. Supposing that the degradation process exactly reaches the threshold at a particular moment t_k, the probability of exceeding the threshold prior to time t_k can be neglected. In this context, the concept of FHT is employed to define the lifespan of the equipment, which can be defined as

$$T = inf\{\, t_k > 0 : X(t_k) \geq W\} \tag{2}$$

Let the RUL of the equipment at time t_k be L_k, which can be expressed as $L_k = T - t_k$. Then the RUL of the equipment at time t_k can be defined as

$$L_k = inf\{\, l_k > 0 : X(t_k + l_k) \geq W | X(t_k) < W\} \tag{3}$$

Where $l_k$denotes the time when the RUL is L_k .

3. Distribution Function of RUL

To estimate the RUL, the analytical expression of the PDF for the degradation model needs to be obtained. In order to obtain the RUL distribution function, three lemmas are introduced.

Lemma 1[40]**.** For a stochastic degradation process $\{X(t), t \geq 0\}$, if $\mu(t; \theta)$ is a continuous function of time *t*. The PDF of the FHT of the degradation process $\{X(t), t \geq 0\}$ to a fixed failure threshold *W* can be written as

$$f_T(t|\Theta) \approx \frac{1}{\sqrt{2\pi t}} \left(\frac{S_B(t)}{t} + \frac{\mu(t;\theta)}{\sigma_B} \right) exp\left(-\frac{S_B^2(t)}{2t} \right) \tag{4}$$

Where $S_B(t) = \frac{\left(W - \int_0^t \mu(\tau;\theta)\, d\tau \right)}{\sigma_B}$, and Θ is the vector of unknown parameters of the model.

Lemma 2[40]**.** If ρ follows a normal distribution with mean $\mu$and variance σ^2, denoted as $\rho \sim N(\mu, \sigma^2)$, $\omega, K_1, K_2 \in R$, and $K_3 \in R^+$, then the following formula is true.

$$E_\rho \left[(\omega - K_1\rho)\, exp\left(-\frac{(\omega - K_2\rho)^2}{2K_3} \right) \right] = \sqrt{\frac{K_3}{K_2^2\sigma^2 + K_3}} \Big(\omega - K_1 \frac{K_2\sigma^2\omega + \mu K_3}{{K_2}^2\sigma^2 + K_3} \Big) \times exp\left(-\frac{(\omega - K_2\mu)^2}{2({K_2}^2\sigma^2 + K_3)} \right) \tag{5}$$

According to Lemma 1, the PDF of the FHT for Model M1

is obtained as

$$f_{T|\nu,\sigma}(t|\nu,\sigma)=\frac{W-\nu\chi(t)}{\sigma\sqrt{2\pi t^3}}exp\left[-\frac{(W-\nu\gamma(t))^2}{2\sigma^2 t}\right] \quad (6)$$

Where $\chi(t)=\int_0^t \Lambda(\tau,b)\,d\,\tau - t\Lambda(t,b)$, $\gamma(t)=\int_0^t \Lambda(\tau,b)\,d\,\tau$.

The degradation value x_k of the PDF of the RUL for model M1 can be given by

$$f_{L_k|\nu,\sigma}(l_k|\nu,\sigma)=\frac{1}{\sqrt{2\pi l_k^3}}(W-x_k-\nu\chi_L(l_k))\,exp\left[-\frac{(W-x_k-\nu\gamma_L(l_k))^2}{2\sigma^2 l_k}\right] \quad (7)$$

Where $\chi_L(l_k)=\int_{t_k}^{l_k+t_k}\Lambda(\tau,b)\,d\,\tau - l_k\Lambda(l_k+t_k,b)$, $\gamma_L(l_k)=\int_{t_k}^{l_k+t_k}\Lambda(\tau,b)\,d\,\tau$.

By considering the individual variability in the degradation process, i.e. assuming the drift coefficient follows a normal distribution, the general formula for the total probability regarding the parameter ν is given by

$$f_{L_k|\sigma}(l_k|\sigma)=\int_\nu f_{L_k|\nu,\sigma}(l_k|\nu,\sigma)\,d\,t=E_\nu\left[f_{L_k|\nu,\sigma}(l_k|\nu,\sigma)\right] \quad (8)$$

According to the assumptions $\delta=1/\sigma^2$, $\sigma_\nu^2=\phi/\delta$, $\nu|\delta\sim N(\mu_\nu,\sigma_\nu^2)$, Lemma 2, Eqs. (6) and (7), when the parameter δ is given, the PDF of the FHT can be expressed as

$$f_{L_k|\delta}(l_k|\delta)=E_{\nu|\delta}\left[f_{L_k|\nu,\delta}(l_k|\nu,\delta)\right]=\frac{1}{\sqrt{2\pi l_k^2(\phi\gamma_L^2(l_k)+l_k)}}\delta^{\frac{1}{2}}\left(W-x_k-\chi(l_k)\frac{(W-x_k)\phi\gamma_L(l_k)+\mu_\nu l_k}{\phi\gamma_L^2(l_k)+l_k}\right)exp\left(-\frac{(W-x_k-\mu_\nu\gamma_L(l_k))^2}{2(\phi\gamma_L^2(l_k)+l_k)}\delta\right) \quad (9)$$

Considering the influence of external random factors on the degradation process, assuming that the diffusion coefficient follows a gamma distribution, the full probability formula with respect to parameter δ can be obtained as

$$f_{L_k}(l_k)=\int_\delta f_{L_k|\delta}(l_k|\delta)dt=E_\delta\left[f_{L_k|\delta}(l_k|\delta)\right] \quad (10)$$

Lemma 3. If ρ follow a Gamma distribution with shape parameter m and scale parameter n, denoted as $\rho\sim Gamma(n,m)$. Then, for $K_1,K_2,a\in R$, the following equation can be obtained.

$$E_\rho[K_1\rho^a\,exp(-K_2\rho)]=\frac{K_1 n^m\Gamma(a+m)}{\Gamma(m)(K_2+n)^{a+m}} \quad (11)$$

Proof of Lemma 3.

$$E_\rho[K_1\rho^a\,exp(-K_2\rho)]=\int_0^{+\infty}K_1\rho^a\,exp(-K_2\rho)\Omega(\rho|m,n)\,d\,\rho$$

$$=\int_0^{+\infty}K_1\rho^a\,exp(-K_2\rho)\frac{n^m}{\Gamma(m)}\rho^{m-1}\,exp(n\rho)\,d\,\rho$$

$$=\frac{K_1 n^m}{\Gamma(m)}\int_0^{+\infty}\rho^{a+m-1}\,exp(-(K_2-n)\rho)\,d\,\rho$$

$$=\frac{K_1 n^m\Gamma(a+m)}{\Gamma(m)(K_2+n)^{a+m}}$$

According to lemma 3 and Eq. (10), the PDF of the RUL for model M1 can be written as

$$f_{L_k}(l_k)=E_\delta\left[f_{L_k|\delta}(l_k|\delta)\right]=\frac{1}{\sqrt{2\pi l_k^2(\phi\gamma_L^2(l_k)+l_k)}}\left(W-x_k-\chi_L(l_k)\frac{(W-x_k)\phi\gamma_L(l_k)+\mu_\nu l_k}{\phi\gamma_L^2(l_k)+l_k}\right)\frac{\beta^\alpha\Gamma\left(\frac{1}{2}+\alpha\right)}{\Gamma(\alpha)\left(\frac{(W-x_k-\mu_\nu\gamma_L(l_k))^2}{2(\phi\gamma_L^2(l_k)+l_k)}+\beta\right)^{\frac{1}{2}+\alpha}} \quad (12)$$

4. Parameter Estimation

The maximum likelihood function of the parameters in the statistical model is derived from the distribution of degradation increments. The expectations in the E-step of the EM algorithm are obtained by updating the posterior distribution. The vector of unknown parameters $\Theta=(\mu_\nu,\phi,b,\alpha,\beta)$ in the PDF of the RUL for model M1 are estimated through the iterations of the extended EM algorithm.

4.1. Likelihood Function

Let t_{ij} denote the time of the *j*th inspection for the *i*th equipment, and $X(t_{ij})=x_{ij}$ denote the measurement value for the *j*th inspection of the *i*th equipment. Here, $i=1,2,\ldots,N$, $j=0,1,2,\ldots,M_i$, and M_i represents the number of monitoring times for the *i*th equipment, and *N* represents the total number of the equipment. In model M1, when parameters ν_i and δ_i are given, according to the properties of the WP, the degradation increment for the *i*th observed sample follows a normal distribution and can be represented as

$$\Delta x_{ij}=x_{ij}-x_{i,j-1}\sim N\left(\nu_i\Delta\tau_{ij},\frac{\Delta t_{ij}}{\delta_i}\right) \quad (13)$$

Where $\Delta t_{ij}=t_{ij}-t_{i,j-1}$ is the time increment and $\Delta\tau_{ij}=\int_{t_{i,j-1}}^{t_{ij}}\Lambda(z,b)dz$ is the nonlinear increment function.

Based on the distribution of degradation increments, when

parameters v_i and δ_i are given, the likelihood function of the ith sample can be expressed as

$$P\left(x_{i,0:M_i} \mid v_i, \delta_i\right) = \prod_{j=1}^{M_i} f\left(\Delta x_{ij} \mid v_i, \delta_i\right)$$

$$= \prod_{j=1}^{M_i} \left\{ \frac{1}{\sqrt{2\pi\Delta t_{ij}}} \delta_i^{\frac{1}{2}} exp\left(-\frac{\left(\Delta x_{ij} - v_i \Delta\tau_{ij}\right)^2}{2\Delta t_{ij}} \delta_i \right) \right\} \quad (14)$$

The likelihood function for v_i and δ_i can be written as

$$L_i(\Theta) = \int_0^{+\infty} \int_{-\infty}^{+\infty} P\left(x_{i,0:M_i} \mid v_i, \delta_i\right) P(v_i \mid \delta_i) P(\delta_i)\, d\,\delta_i\, d\,v = \frac{\beta^\alpha \Gamma\left(\frac{M_i}{2}+\alpha\right)}{\Gamma(\alpha)\sqrt{\Delta w_{i,M_i}\phi+1}(2\pi)^{\frac{M_i}{2}} \prod_{j=1}^{M_i}(\Delta t_{ij})^{\frac{1}{2}} \left(\frac{\Delta c_{i,M_i}}{2} + \frac{\mu_a^2}{2\phi} - \frac{\left(\Delta d_{i,M_i}\phi+\mu_v\right)^2}{2\phi\left(\Delta w_{i,M_i}\phi+1\right)} + \beta \right)^{\frac{M_i}{2}+\alpha}} \quad (17)$$

Where $\Delta c_{i,M_i} = \sum_{j=1}^{M_i} \left(\frac{\Delta x_{ij}^2}{\Delta t_{ij}} \right)$, $\Delta d_{i,M_i} = \sum_{j=1}^{M_i} \frac{\Delta x_{ij}\Delta\tau_{ij}}{\Delta t_{ij}}$, $\Delta w_{i,M_i} = \sum_{j=1}^{M_i} \frac{\Delta\tau_{ij}^2}{\Delta t_{ij}}$.

$$P(v_i \mid \delta_i) = \prod_{j=1}^{M_i} f(v_i \mid \delta_i) = \prod_{j=1}^{M_i} \left\{ \frac{1}{\sqrt{2\pi\phi}} \delta_i^{\frac{1}{2}} exp\left[-\frac{(v_i-\mu_v)^2}{2\phi} \delta_i \right] \right\} \quad (15)$$

$$P(\delta_i) = \prod_{j=1}^{M_i} f(\delta_i) = \prod_{j=1}^{M_i} \left\{ \frac{\beta^\alpha}{\Gamma(\alpha)} \delta_i^{\alpha-1} exp(\beta\delta_i) \right\} \quad (16)$$

Since $v|\delta \sim N(\mu_v, \frac{\phi}{\delta})$, $\delta \sim Gamma(\alpha, \beta)$, according to the distribution of the degradation increment Δx_{ij}, the likelihood function of the ith sample represented by the degradation increment Δx_{ij} is

After obtaining the likelihood function $L_C(\Theta) = \prod_{i=1}^{N} L_i(\Theta)$ of the complete data, the log-likelihood function can be obtained by taking the logarithm on both sides as

$$ln\, L_C(\Theta) = \sum_{i=1}^{N} \sum_{j=1}^{M_i} \left[\frac{1}{2} ln\, \delta_i - \frac{1}{2} ln(2\pi) - \frac{1}{2} ln\left(\Delta t_{ij}\right) - \frac{\left(\Delta x_{ij} - v_i \Delta\tau_{ij}\right)^2}{2\Delta t_{ij}} \delta_i \right] + \sum_{i=1}^{N} \left[\frac{1}{2} ln\, \delta_i - \frac{1}{2} ln(2\pi) - \frac{1}{2} ln\, \phi - \frac{(v_i-\mu_v)^2}{2\phi} \delta_i \right] +$$
$$\sum_{i=1}^{N} [\alpha\, ln\, \beta - ln\, \Gamma(\alpha) + (\alpha-1)\, ln(\delta_i) - \beta\delta_i] \quad (18)$$

4.2. The Posterior Distribution Update

Based on $v|\delta \sim N(\mu_v, \frac{\phi}{\delta})$, $\delta \sim Gamma(\alpha, \beta)$ and Bayesian formula, the posterior distribution of parameters v_i, δ_i can be expressed as

$$P\left(v_i \mid x_{i,0:M_i}, \delta_i\right) = \frac{P\left(x_{i,0:M_i} | v_i, \delta_i\right) P(v_i|\delta_i) P(\delta_i)}{P\left(x_{i,0:M_i}, \delta_i\right)} \propto P\left(x_{i,0:M_i} \mid v_i, \delta_i\right) \cdot P(v_i \mid \delta_i) \cdot P(\delta_i) \propto exp\left[-\frac{\left(v_i - \frac{\Delta d_{i,M_i}\phi+\mu_v}{\Delta w_{i,M_i}\phi+1} \right)^2}{\frac{2\phi}{\left(\Delta w_{i,M_i}\phi+1\right)}} \delta_i \right] \quad (19)$$

$$P\left(\delta_i \mid x_{i,0:M_i}\right) = \frac{P\left(x_{i,0:M_i} | \delta_i\right) P(\delta_i)}{P\left(x_{i,0:M_i}\right)} \propto \int_{-\infty}^{+\infty} P\left(x_{i,0:M_i} \mid v_i, \delta_i\right) P(v_i \mid \delta_i) dv_i P(\delta_i) \propto \delta_i^{\frac{M_i}{2}+\alpha-1} exp\left\{ -\left[\frac{\Delta c_{i,M_i}}{2} + \frac{\mu_v^2}{2\phi} - \frac{\left(\Delta d_{i,M_i}\phi+\mu_v\right)^2}{2\phi\left(\Delta w_{i,M_i}\phi+1\right)} + \beta \right] \delta_i \right\} \quad (20)$$

So the posterior distribution of parameters v_i and δ_i can be rewritten as

$$v_i \mid x_{i,0:M_i}, \delta_i \sim N\left(\frac{\Delta d_{i,M_i}\phi+\mu_v}{\Delta w_{i,M_i}\phi+1}, \frac{\phi}{\left(\Delta w_{i,M_i}\phi+1\right)\delta_i} \right) \quad (21)$$

$$\delta_i \mid x_{i,0:M_i} \sim Gamma\left(\alpha + \frac{M_i}{2}, \frac{\Delta c_{i,M_i}}{2} + \frac{\mu_v^2}{2\phi} - \frac{\left(\Delta d_{i,M_i}\phi+\mu_v\right)^2}{2\phi\left(\Delta w_{i,M_i}\phi+1\right)} + \beta \right) \quad (22)$$

According to Eqs. (21) and (22), by using the variance formula, the expectations of v_i, δ_i, v_i^2 and $ln\, \delta_i$ are

$$E\left(v_i \mid x_{i,0:M_i}, \delta_i\right) = \frac{\Delta d_{i,M_i}\phi+\mu_v}{\Delta w_{i,M_i}\phi+1} \quad (23)$$

$$E\left(\delta_i \mid x_{i,0:M_i}\right) = \frac{\alpha+\frac{M_i}{2}}{\frac{\Delta c_{i,M_i}}{2} + \frac{\mu_v^2}{2\phi} - \frac{\left(\Delta d_{i,M_i}\phi+\mu_v\right)^2}{2\phi\left(\Delta w_{i,M_i}\phi+1\right)} + \beta} \quad (24)$$

$$E\left(v_i^2 \mid x_{i,0:M_i}, \vartheta_i\right) = E^2\left(v_i \mid x_{i,0:M_i}, \delta_i\right) + Var\left(v_i \mid x_{i,0:M_i}, \delta_i\right) = \left(\frac{\Delta d_{i,M_i}\phi+\mu_v}{\Delta w_{i,M_i}\phi+1} \right)^2 + \frac{\phi}{\left(\Delta w_{i,M_i}\phi+1\right)\delta_i} \quad (25)$$

$$E\left(ln\, \delta_i \mid x_{i,0:M_i}\right) = \psi\left(\alpha + \frac{M_i}{2}\right) - ln\left[\frac{\Delta c_{i,M_i}}{2} + \frac{\mu_v^2}{2\phi} - \frac{\left(\Delta d_{i,M_i}\phi+\mu_v\right)^2}{2\phi\left(\Delta w_{i,M_i}\phi+1\right)} + \beta \right] \quad (26)$$

Where $\psi(\bullet)$ is the digamma function. In order to obtain the expectation of the log-likelihood function used in the EM algorithm, Eqs. (23) to (26) can be rewritten as

$$E_{1i}(\Theta) = E\left(v_i \mid x_{i,0:M_i}, \delta_i\right) \qquad E_{2i}(\Theta) = \frac{\phi}{\left(\Delta w_{i,M_i}\phi+1\right)}$$
$$E_{3i}(\Theta) = E\left(\delta_i \mid x_{i,0:M_i}\right) \qquad E_{4i}(\Theta) = E\left(ln\, \delta_i \mid x_{i,0:M_i}\right) \quad (27)$$

The above expectations and related definitions can be used to calculate the expectation function of the E-step in the EM

algorithm.

4.3. EM Algorithm Parameter Estimation

E-step. The latent variable is estimated by calculating the expected value at this step. The result of the *k*th iteration of the unknown parameter vector is denoted as $\Theta^{(k)} = \left(\mu_v{}^{(k)}, \phi^{(k)}, b^{(k)}, \alpha^{(k)}, \beta^{(k)}\right)$. The expectation of the log-likelihood function of the complete data under the condition of the measured equipment degradation data $X_{1:N,0:M_i}$ and the estimated value $\Theta_1^{(k)}$ after the *k*th iteration is

$$Q\left(\Theta \mid X_{1:N,0:M_i}, \Theta^{(k)}\right) = \sum_{i=1}^{N}\sum_{j=1}^{M_i}\left\{\frac{1}{2}E_{4i}\left(\Theta^{(k)}\right) - \frac{1}{2}ln(2\pi) - \frac{1}{2}ln\left(\Delta t_{ij}\right) - \left[\frac{\Delta x_{ij}^2}{2\Delta t_{ij}}E_{3i}\left(\Theta^{(k)}\right) - \frac{\Delta x_{ij}\Delta\tau_{ij}}{\Delta t_{ij}}E_{1i}\left(\Theta^{(k)}\right)E_{3i}\left(\Theta^{(k)}\right) + \right.\right.$$

$$\left.\left.\frac{\Delta\tau_{ij}{}^2}{2\Delta t_{ij}}\left[E_{1i}^2\left(\Theta^{(k)}\right) + \frac{E_{2i}\left(\Theta^{(k)}\right)}{E_{3i}\left(\Theta^{(k)}\right)}\right]E_{3i}\left(\Theta^{(k)}\right)\right]\right\} + \sum_{i=1}^{N}\left\{\frac{1}{2}E_{4i}\left(\Theta^{(k)}\right) - \frac{1}{2}ln(2\pi) - \frac{1}{2}ln\,\phi - \left[\frac{\mu_v{}^2}{2\varphi}E_{3i}\left(\Theta^{(k)}\right) - \frac{\mu_v}{\varphi}E_{1i}\left(\Theta^{(k)}\right)E_{3i}\left(\Theta^{(k)}\right) + \right.\right.$$

$$\left.\left.\frac{1}{2\varphi}\left[E_{1i}^2\left(\Theta^{(k)}\right) + \frac{E_{2i}\left(\Theta^{(k)}\right)}{E_{3i}\left(\Theta^{(k)}\right)}\right]E_{3i}\left(\Theta^{(k)}\right)\right]\right\} + \sum_{i=1}^{N}\left[\alpha\,ln\,\beta - ln\,\Gamma(\alpha) + (\alpha-1)E_{4i}\left(\Theta^{(k)}\right) - \beta E_{3i}\left(\Theta^{(k)}\right)\right] \quad (28)$$

M-step. The central goal in this step is to find the maximum of function $Q\left(\Theta \mid X_{1:N,0:M_i}, \Theta^{(k)}\right)$ with respect to Θ. It can be written as

$$\hat{\Theta}^{(k+1)} = arg\max_{\Theta}\left\{Q\left(\Theta \mid X_{1:N,0:M_i}, \Theta^{(k)}\right)\right\} \quad (29)$$

To obtain the parameter values after the *k*+1th iteration, Eq.(28) is differentiated with respect to the parameters Θ and the five resulting expressions are set to zero. Eq.(28) can be expressed as

$$\begin{cases} \frac{\partial Q}{\partial \mu_v} = -\sum_{i=1}^{N}\left[\frac{\mu_v}{\phi}E_{3i}\left(\Theta^{(k)}\right) - \frac{E_{1i}\left(\Theta^{(k)}\right)E_{3i}\left(\Theta^{(k)}\right)}{\phi}\right] = 0 \\ \frac{\partial Q}{\partial \phi} = \sum_{i=1}^{N}\left\{-\frac{1}{2\phi} - \left[-\frac{\mu_v{}^2}{2\phi^2}E_{3i}\left(\Theta^{(k)}\right) + \frac{\mu_v}{\phi^2}E_{1i}\left(\Theta^{(k)}\right)E_{3i}\left(\Theta^{(k)}\right) - \right.\right. \\ \left.\left.\frac{E_{1i}^2\left(\Theta^{(k)}\right)E_{3i}\left(\Theta^{(k)}\right)}{2\phi^2} - \frac{E_{2i}\left(\Theta^{(k)}\right)}{2\phi^2}\right]\right\} = 0 \\ \frac{\partial Q}{\partial b} = \sum_{i=1}^{N}\sum_{j=1}^{M_i}\left\{\frac{\Delta x_{ij}\Delta\tau_{ij}}{\Delta t_{ij}}E_{1i}\left(\Theta^{(k)}\right)E_{3i}\left(\Theta^{(k)}\right) - \right. \\ \left.\left.\frac{\Delta\tau_{ij}{}^2}{2\Delta t_{ij}}\left[E_{1i}^2\left(\Theta^{(k)}\right)E_{3i}\left(\Theta^{(k)}\right) + E_{2i}\left(\Theta^{(k)}\right)\right]\right\}\right|_b{}' = 0 \\ \frac{\partial Q}{\partial \alpha} = \sum_{i=1}^{N}\left[ln\,\beta - \psi(\alpha) + E_{4i}\left(\Theta^{(k)}\right)\right] = 0 \\ \frac{\partial Q}{\partial \beta} = \sum_{i=1}^{N}\left[\frac{\alpha}{\beta} - E_{3i}\left(\Theta^{(k)}\right)\right] = 0 \end{cases} \quad (30)$$

In the third formula of Eq.(30), the derivative expression of parameter *b* cannot be explicitly expressed, and it can be solved by using the fsolve function in MATLAB. Then the results of the parameters Θ in Eq.(30) after the *k*+1th iteration can be obtained as

$$\mu_v^{(k+1)} = \frac{\sum_{i=1}^{N}\left[E_{1i}\left(\Theta^{(k)}\right)E_{3i}\left(\Theta^{(k)}\right)\right]}{\sum_{i=1}^{N}E_{3i}\left(\Theta^{(k)}\right)} \quad (31)$$

$$\phi^{(k+1)} = \frac{1}{N} + \sum_{i=1}^{N}E_{1i}^2\left(\Theta^{(k)}\right)E_{3i}\left(\Theta^{(k)}\right) + \sum_{i=1}^{N}E_{2i}\left(\Theta^{(k)}\right)\} \quad (32)$$

$$\sum_{i=1}^{N}\sum_{j=1}^{M_i}\left\{\frac{\Delta x_{ij}\Delta\tau_{ij}}{\Delta t_{ij}}E_{1i}\left(\Theta^{(k)}\right)E_{3i}\left(\Theta^{(k)}\right) - \frac{\Delta\tau_{ij}{}^2}{2\Delta t_{ij}}\left[E_{1i}^2\left(\Theta^{(k)}\right)E_{3i}\left(\Theta^{(k)}\right) + E_{2i}\left(\Theta^{(k)}\right)\right]\right\}\Big|_b{}' = 0 \quad (33)$$

$$\sum_{i=1}^{N}\left\{ln\,N + ln\,\alpha - ln\left[\sum_{i=1}^{N}E_{3i}\left(\Theta^{(k)}\right)\right] - \psi(\alpha) + E_{4i}\left(\Theta^{(k)}\right)\right\} = 0 \quad (34)$$

$$\beta^{(k+1)} = \frac{N\alpha^{(k+1)}}{\sum_{i=1}^{N}E_{3i}\left(\Theta^{(k)}\right)} \quad (35)$$

A better estimation value can be obtained after a certain number of iterations. By substituting the estimation results into the PDFs of RUL, the exact expressions of the RUL can be obtained. The flowchart of the EM algorithm is shown in Fig. 1.

5. Experimental Investigations

The model proposed in this paper is designated as model M1, and the work of Si et al.[40] is denoted as Model M2, which only takes into account the individual differences random effect of the drift coefficient. The degradation model can be expressed as

$$X(t_k) = X(0) + \nu\int_0^{t_k}\Lambda(z,b)\,\mathrm{d}z + \sigma B(t_k) \quad (36)$$

Where the drift coefficient ν follows a normal distribution with mean μ_ν and variance σ_ν^2, denoted as $\nu \sim N(\mu_\nu, \sigma_\nu^2)$. The nonlinear function $\int_0^{t_k}\Lambda(z,b)\,dz = \mu(t_k;b)$ is the same as that in M1, while the diffusion coefficient σ is fixed in M2. Thus, the unknown parameters of M2 can be denoted as $\Theta_1 = (\mu_\nu, \sigma_\nu, b, \sigma)$. By employing two performance metrics, the proposed model is compared with the models existing in previous studies to assess the performance of RUL estimation. Meanwhile, the two performance metrics are Akaike Information Criterion (AIC) criterion and the Total Mean

Square Error (TMSE). The AIC is utilized to prevent over-parameterization and achieve a balance between model complexity and fitting accuracy. A smaller AIC value implies better model performance[41].

$$AIC = -2\,max\,\ell + 2p \tag{37}$$

Where $max\,\ell$ is the maximum log-likelihood function (Log-LF) value, p is the total number of parameters. In addition, the Mean Square Error (MSE) is defined as the expectation of the difference between the actual RUL and the estimated RUL at each monitoring point. A smaller MSE indicates a more accurate estimate. The TMSE is the sum of the squared differences between the estimated RUL and the actual RUL for all the monitoring points, and can be expressed as

$$TMSE = \sum_{k=1}^{N} E\left((L_k - \tilde{L}_k)^2\right) \tag{38}$$

Where $L_k, \tilde{L}_k$ is the actual RUL and the estimated RUL at t_k, and N is the number of all samples. In order to conduct a more in-depth comparison, the following two data-sets are utilized for experimental investigations.

5.1. XJTU-SY Rolling Bearing Accelerated Life Test Dataset

The XJTU-SY rolling bearing dataset is acquired from the testbed depicted in Fig. 1. The platform comprises an AC motor, a motor speed controller, a rotating shaft, support bearings, and other components. This platform is capable of performing accelerated degradation tests on bearings to provide real experimental data that characterize the degradation of bearings throughout their entire operating lifespan. The tested bearing type is LDK UER204, and three different operating conditions are applied to 15 bearings. The DT9837 portable dynamic signal collector is utilized to collect horizontal and vertical vibration signals.

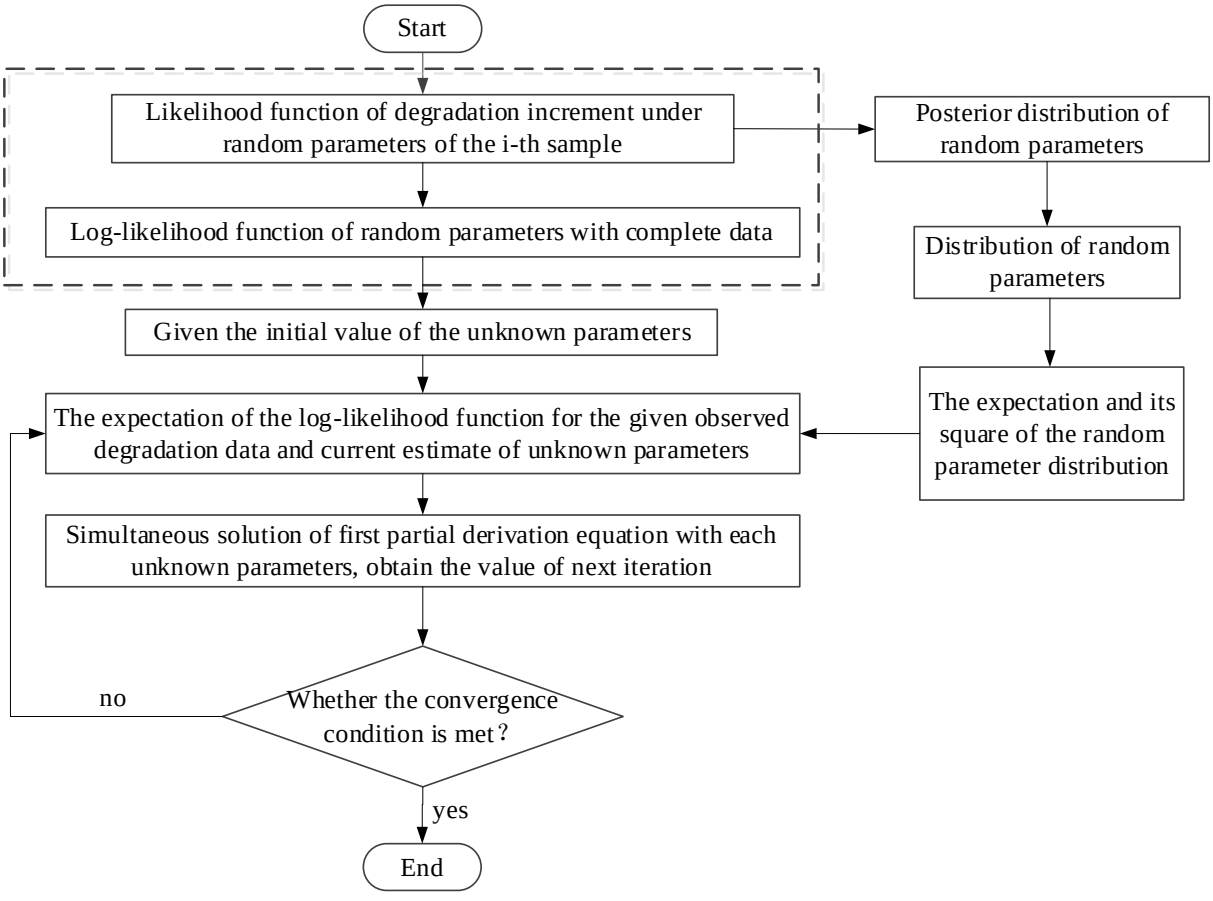

Figure 1. Flowchart of the extended EM algorithm.

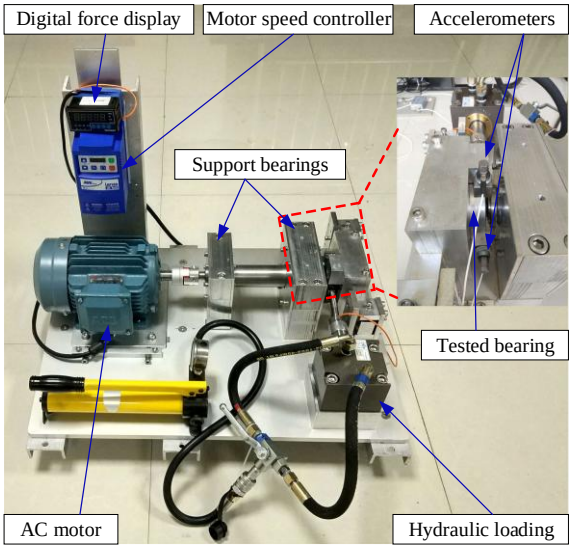

Figure 2. Bearing testbed[42].

The information regarding the total number of samples, basic rated life L_{10}, actual life under the first operating condition is listed in Table 1. According to the national standard, the basic rated life L_{10} is the life that a group of bearings of the same type can reach or exceed under identical conditions with a reliability of 90%[42]. The operating conditions of the test bearings are a rotational speed of 2100 r/min and a radial force of 12 KN. For further details, refer to reference [42].

Table 1. Information of XJTU-SY rolling bearing dataset[42].

Total number of samples	L_{10}	actual life	Data-set
123		2h3min	Bearing 1_1
161		2h41min	Bearing 1_2
158	5.6~9.7 h	2h38min	Bearing 1_3
122		2h2min	Bearing 1_4
52		52min	Bearing 1_5

To represent the degradation process from the normal state to the failure state, signal processing techniques are typically employed to extract features from the time domain, frequency domain, and time-frequency domain during the entire operating life of a bearing. For instance, the typical horizontal vibration signals throughout the operating life are selected to illustrate the degradation process. Fig.3 displays the horizontal vibration signal of bearing 1_1. To depict the performance degradation process more intuitively, the Hilbert transform is applied to calculate the envelope of the vibration amplitude. It is evident that the amplitude increases with the running time, particularly in the final stage of the operating period. The relative method is utilized to determine the failure threshold of the bearing, i.e. when the maximum value of the vibration signal exceeds $10 \times A_h$, where A_h is the maximum value of the bearing during the normal operation stage.

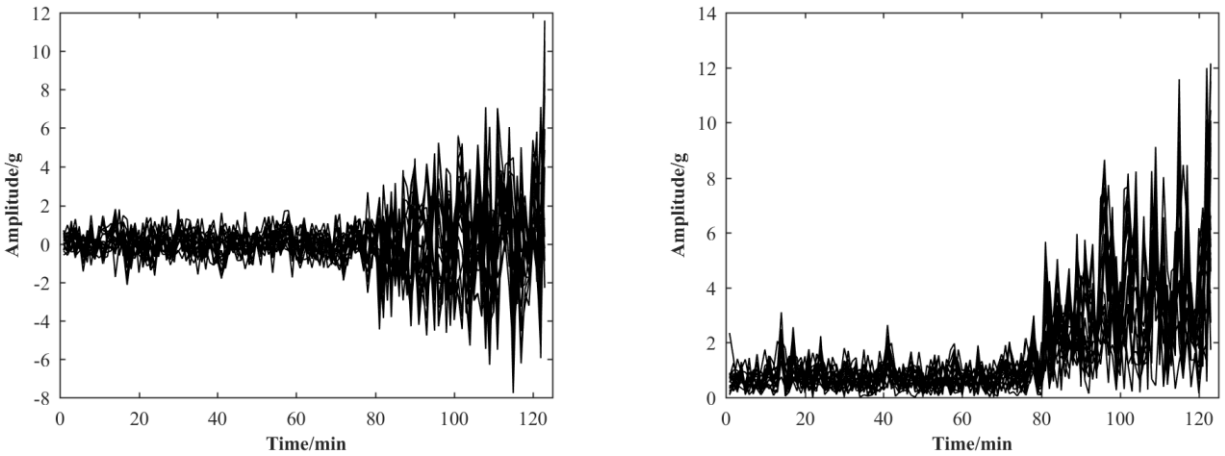

Vibration amplitude of bearing 1_1 (b) Vibration amplitude after Hilbert transform

Figure 3. Typical horizontal vibration signals.

Interference signals and noise are commonly present in the monitoring data and accumulate during the data collection process. These signals and noise can affect the accuracy of the estimation results. The moving average method is selected to reduce the noise of the data-sets, due to its easy implementation and wide usage. To obtain the development trend of the whole data, the data are shifted backward one by one according to the given filter window width and the existing time series. The measurement values of adjacent times are added and averaged as follows

$$p_t = \frac{\sum_{i=1}^{n}(x_{t-i}+x_{t+i})+x_t}{2n+1} \tag{39}$$

Where p_t is the filtering result, x_m is the true degradation value at time m, and n is the filter window width. The sliding window is an important parameter in the moving average filtering. The smaller the sliding window, the higher the sensitivity; while the larger the sliding window, the more obvious the smoothing effect, making the trend of data change more distinct.

Take bearing 1_3 as an example, the filtering result of the vibration signal is shown in Fig. 4(a). After filtering, the quality and reliability of the signals are improved, making the degradation trends more intuitive. The processed results of the monitoring data for the 5 test bearings of dataset bearing 1 are shown in Fig. 4(b). The result shows that the life varies among individuals. It further demonstrates the necessity of considering individual differences in the model.

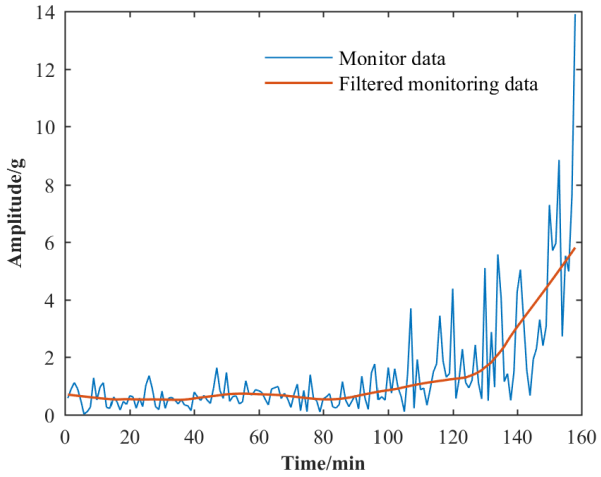

(a) Comparison of signal before and after filter

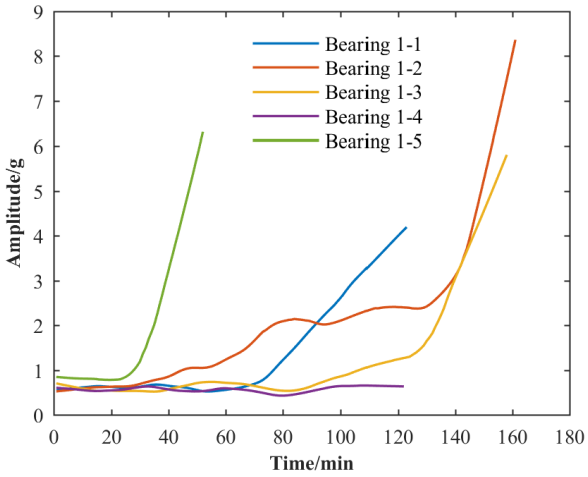

(b) The vibration signal of bearings 1-5 after filter

Figure 4. Filtering results of the vibration signal.

Due to individual differences, the test life of the bearings in dataset 1 is significantly different. In order to verify the model more clearly, the vibration signal data of the third bearing of dataset 1 is taken as the verification data of the model. The actual life of the third bearing is 158 minutes, and the failure threshold of amplitude is 8, calculated by using the relative method mentioned above. In addition, nonlinear functions can take various forms, including polynomials, exponential functions, and power functions. By observing the degradation curve, the exponential function is selected as the nonlinear function for calculations in the experimental studies of this paper, i.e. $\Lambda(t;b) = b\,exp\,b\,t$. The unknown parameters are estimated by using the extended EM algorithm introduced above. Table 2 shows the comparison of the estimated parameter values and the performance evaluation index values of different models.

Table 2. Comparisons of different Models with XJTU-SY rolling bearing data.

Model	μ_v	σ_v	ϕ	b	α	β	*Log-LF*	*AIC*	*TMSE*
M1	2.1686E-11	-	1.4771E-14	1.0369	1.0862	4.0880	*69*	*-128*	*6.2014*
M2	1.1452E-13	7.4338	-	1.0218	-	-	32	-56	8.0672

It can be seen from the estimated results in Table 2 that the value of log-LF of M1 is greater than that of M2, and the AIC of M1 is smaller than that of M2. Meanwhile, the value of TMSE of M1 is smaller. The results of these three aspects show that the performance of M1 is better than that of M2. In order to further compare the performance of RUL estimation, the PDFs

of different operating times are analyzed.

The estimated parameter results are used to calculate the RULs of the PDFs for the models. The RUL PDFs curves for different operating times are shown in Fig. 5. The figure depicts the RUL PDFs curves for the third bearing of dataset bearing 1. From the figure, it can be observed that as the operating time increases, the RUL PDFs curves become narrower and taller, indicating a more concentrated distribution of the RUL and reduced uncertainty in the estimations. The true RUL values consistently fall within the estimated RUL distributions, validating the effectiveness of the proposed method.

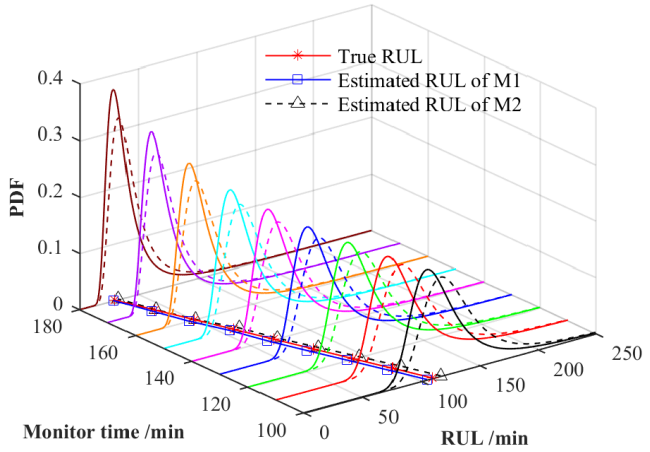

Figure 5. Comparison of the PDFs of the RULs under M1 and M2 with rolling bearing dataset.

5.2. C-MAPSS Turbofan Aero-engine Degradation Simulation Dataset

Aero-engines are one of the most critical components of an aircraft and serve as a key guarantee for flight safety. The overall condition of the engine is not only related to the health status of its individual components but also influenced by various factors such as the aircraft's operating environment, load, usage patterns, and maintenance quality. In this paper, an aero-engine dataset provided by NASA is utilized. It is derived from the Commercial Modular Aero-Propulsion System Simulation (C-MAPSS) for a large-scale turbofan engine simulation. The simulation primarily emulates the degradation process of five significant rotating components, including the fan, low-pressure turbine (LPT), low-pressure compressor (LPC), high-pressure turbine (HPT), and high-pressure compressor (HPC)[5]. The schematic diagram of the engine is illustrated in Fig. 6.

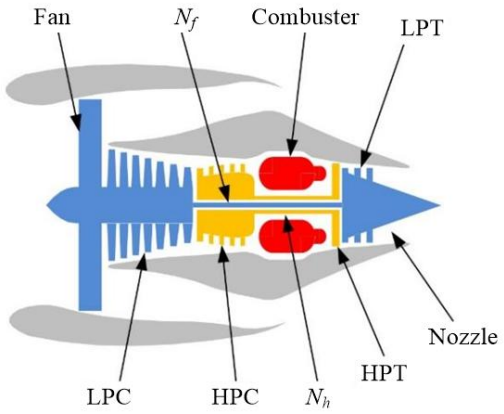

Figure 6. Schematic diagram of an aero-engine[18].

The C-MAPSS dataset consists of four parts, i.e., FD001 to FD004, each comprising a training set and a test set. The initial state of each dataset is randomized, and the testing stops when an engine failure occurs. The dataset has a total of 26 columns, and columns 6 to 26 record the measurements values of monitored sensor with added noise. The descriptions of some sensors are provided in Table 1 (See more details in [18]).

Table 3. Description of some aero-engine sensors[18].

Number	Symbol	Illustrate	Unit
1	T2	Total fan inlet temperature	°R
2	T24	LPC outlet temperature	°R
3	T30	HPC outlet temperature	°R
4	T50	LPT outlet temperature	°R
5	P2	Fan inlet pressure	psia
6	P15	Culvert pressure	psia
7	P30	HPC outlet pressure	psia
8	N_f	Fan speed	rpm

In the C-MAPSS dataset, different sensors exhibit different degradation trends. Selecting sensors with obvious degradation trends for the estimation of RUL is more conducive to model validation and yields more reliable calculation results. In this paper, the multi-dimensional monitoring values of the sensors from 16 engine groups in the FD001 training set are converted into one dimensional performance indicators to reflect the health status of the aero-engine. The FD001 data-set consists of monitoring results from 100 engines, comprising a total of 20,631 data entries. The engine operates in cycles, with a minimum lifespan of 128 cycles and a maximum lifespan of 378 cycles.

As described before, the initial data has great random characteristics, and a large number of random noises are added to each monitoring data. In addition, interference signals are

commonly present in the measurement data and accumulate during the data collection process. It is necessary to pre-process the initial data of the dataset.

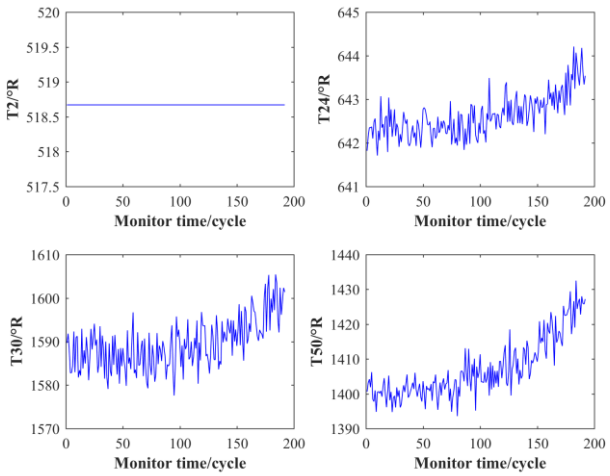

Figure 7. Monitoring data from different sensors.

It is more beneficial and reliable to select the sensor with an obvious degradation tendency for estimating the RUL. Sensors 1# to 4#, namely T2, T24, T30 and T50 were chosen for analysis. The monitoring data of these four sensors is shown in Fig. 7. It can be observed that the monitoring data of each sensor exhibits different degradation trends. The value of the T2 sensor does not change with the operation of the engine. The concept of the Spearman Rank Correlation Coefficient (SRCC) [43] is introduced to evaluate the magnitude of the degradation trend of the remaining three sensors. The SRCC range is [-1,1], where -1 indicates a complete negative correlation, 0 indicates no correlation, and 1 indicates a complete positive correlation. The closer the SRCC is to 1 or -1, the stronger the degradation trend, while the closer it is to 0, the weaker the no degradation trend. The SRCC ρ^i of sensor i is expressed as

$$\rho^i = \frac{\left|\sum_{k=1}^{K}(T_k-\bar{T}_{1:k})(X_k^i-\bar{X}_{1:k}^i)\right|}{\sqrt{\sum_{k=1}^{K}(T_k-\bar{T}_{1:k})^2\sum_{K=1}^{K}(X_k^i-\bar{X}_{1:k}^i)^2}} \tag{40}$$

Where X_k^i is the kth monitoring value of the ith sensor, $\bar{X}_{1:k}^i$ is the average monitoring value of the ith sensor from 1 to k, T_k is the kth monitoring time, and $\bar{T}_{1:k}$ is the average monitoring time from 1 to k. The SRCC values of different sensors are listed in Fig. 8. After analysis, the sensor with an SRCC greater than 0.8 can be used as the performance index of the aero-engines. The measurement results from the T50 sensor of 16 aero-engines in FD001 dataset are selected as the performance monitoring index.

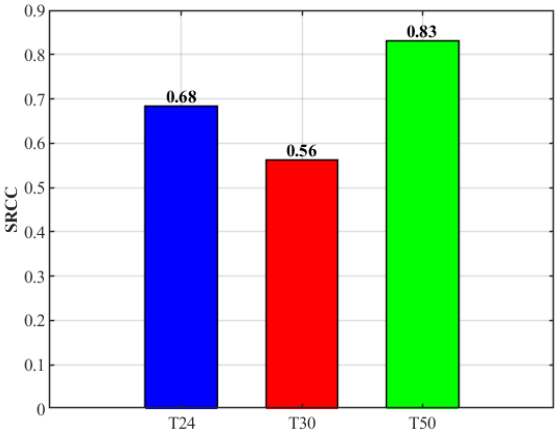

Figure 8. The SRCC of different sensors.

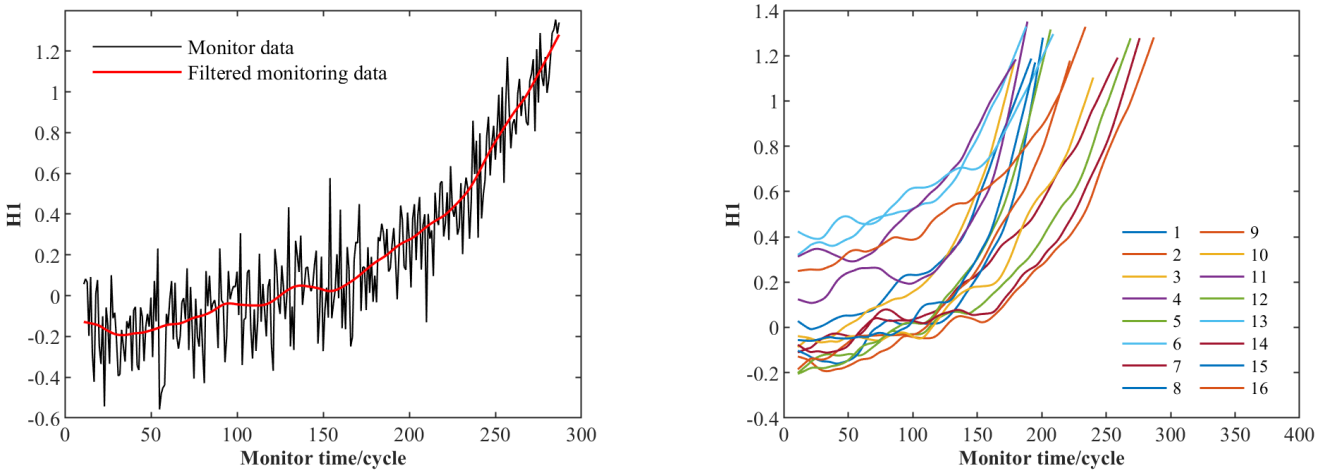

(a) Filter results of the sensors (b) Degradation trend of engines No. 1-16

Figure 9. Filtering results of the sensors.

To reduce the order of magnitude of the whole life cycle degradation data and facilitate the calculation, the mean value of the first ten cycles is subtracted. Moreover, the multi-dimensional measurement values are converted into one-

dimensional performance indicators to reflect the health status. The life of the aero-engines is defined as 200 cycles, and the failure threshold is set at 1423.4 °R. In this paper, the filter window width of the moving average method is set as 30, and one of the data filtering results is shown in Fig. 9. After filtering, noise and sharp signals are removed, making the degradation trends more apparent.

The performance comparison of different models conducted on aero-engines is shown in Table 4. A conclusion similar to that of bearing dataset was obtained. The results of log-LF, AIC and TMSE still indicate that the performance of M1 is better than that of M2. In addition, it could be observed from the comparison between Table 2 and Table 4 that the parameter value of ϕ of the XJTU-SY rolling bearing data in Table 2 are significantly smaller than that in Table 4.

Table 4. Comparisons of different Models with C-MAPSS aero-engine data.

Model	μ_v	σ_v	ϕ	b	α	β	σ	*Log-LF*	*AIC*	*TMSE*
M1	0.3922	-	0.9401	0.0206	93.5738	3.1101	-	*767*	*-1524*	*0.7882*
M2	0.2789	0.1464	-	0.3108	-	-	0.3738	433	-958	1.0421

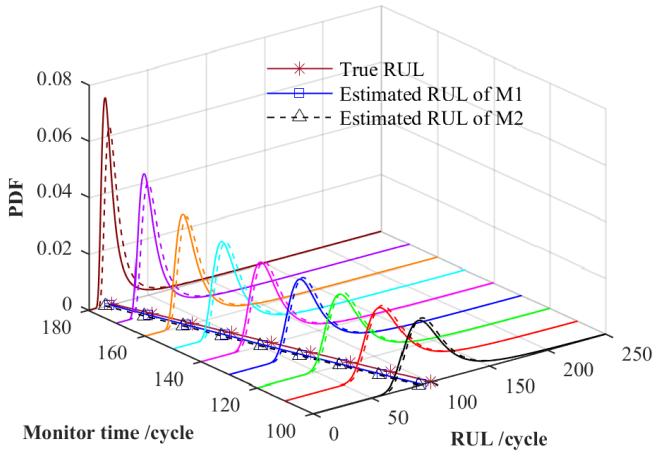

Figure 10. Comparison of the PDFs of the RULs under M1 and M2 with aero-engine data.

This indicates that the range of operating conditions of the samples in the XJTU-SY rolling bearing data is not extensive enough to fully activate the optimization and adjustment mechanisms of all parameters in M1. The significant advantages of M1, which considers individual differences, external random effects and their coupling relationship, are further verified by C-MAPSS aero-engine data. Fig. 10 depicts the RUL PDFs curves for the aero-engines operating from 100 cycles to 180 cycles, as well as the estimated RUL and true RUL for each operating cycle. From the figure, it can be seen that the RUL PDF curve of M1 is narrower and taller compared to that of M2. This implies that the estimations of M1 are more concentrated and have lower uncertainty, resulting in a better performance in RUL estimation. By comparing the TMSE of the true and estimated RUL values, it can be concluded that the estimations of M1 are closer to the true values. To further validate the accuracy of M1, the fitting results of M1 are compared with the actual degradation curves, as illustrated in Fig. 11. From the figure, it can be seen that the fitting curve of M1 closely approximates the true average degradation curve, thereby attesting to the accuracy and effectiveness of the model presented in this paper.

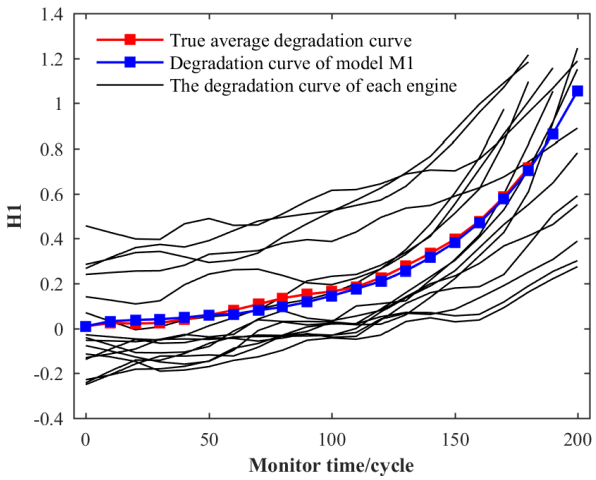

Figure 11. Fitting curve of M1.

6. Conclusions

The nonlinear WP degradation model proposed in this paper shows high RUL estimation accuracy, which proves its effectiveness under various equipment degradation conditions. The proposed model precisely captures individual differences, external random factors and their coupling, providing a more realistic portrayal of the degradation process. The comprehensive RUL estimation method was verified using the datasets of rolling bearings and aero- engines. This involves the

detailed procedures of deriving the analytical expression of the PDF of the model's RUL considering the FHT and conducting parameter estimation using the extended EM algorithm. This paper lays a foundation for the development of degradation model addressing the coupling of multiple factors, thus promoting the progress of PHM.

The proposed nonlinear WP degradation model shows high RUL estimation accuracy, which proves its effectiveness under various equipment degradation conditions.

The development of degradation model addressing the coupling of multiple factors

The comprehensive RUL estimation method was verified using the datasets of rolling bearings and aero-engines.

Acknowledgement

This work is supported by the National Natural Science Foundation of China (Grant No. 52075438), Key Research and Development Program of Shaanxi Province of China (Grant No. 2024GX-YBXM-268).

References

1. Hu Y, Miao XW, Si Y, Pan E, Zio E. Prognostics and health management: A review from the perspectives of design, development and decision. Reliability Engineering and System Safety 2022; 217: 108063, https://doi.org/10.1016/j.ress.2021.108063.
2. Zhang ZX, Si XS, Hu CH, Lei YG. Degradation data analysis and remaining useful life estimation: A review on Wiener-process-based methods. European Journal of Operational Research 2018; 271: 775-796, https://doi.org/10.1016/j.ejor.2018.02.033.271:775-796
3. Zhang SJ, Kang R, Lin YH. Remaining useful life prediction for degradation with recovery phenomenon based on uncertain process. Reliability Engineering and System Safety 2021; 208: 107440, https://doi.org/10.1016/j.ress.2021.107440.
4. Ellefsen AL, Bjørlykhaug E, Æsøy V, Ushakov S, Zhang HX. Remaining useful life predictions for turbofan engine degradation using semi-supervised deep architecture. Reliability Engineering and System Safety 2019; 183: 240-251, https://doi.org/10.1016/j.ress.2018.11.027.
5. Liu L, Song X, Zhou ZT. Aircraft engine remaining useful life estimation via a double attention-based data-driven architecture. Reliability Engineering and System Safety 2022; 221: 108330, https://doi.org/10.1016/j.ress.2022.108330
6. Zhang YH, Yang Y, Li H, Xiu XC, Liu WQ. A data-driven modeling method for stochastic nonlinear degradation process with application to RUL estimation. IEEE Transactions on Systems, Man, and Cybernetics: Systems 2022; 52(6): 3847-3858, https://doi.org/10.1109/TSMC.2021.3073052.
7. Zeng LQ, Zheng JH, Yao L, Ge ZQ. Dynamic Bayesian networks for feature learning and transfer applications in remaining useful life estimation. IEEE Transactions on Instrumentation and Measurement 2023; 72: 3500312, https://doi.org/10.1109/TIM.2022.3221142
8. Wu JY, Wu M, Chen ZH, Li XL, Yan RQ. A joint classification-regression method for multi-stage remaining useful life prediction. Journal of Manufacturing Systems 2021; 58: 109-119, https://doi.org/10.1016/j.jmsy.2020.11.016.
9. Liang ZM, Gao JM, Jiang HQ, Gao X, Gao ZY, Wang RX. A similarity-based method for remaining useful life prediction based on operational reliability. Applied Intelligence 2018; 48: 2983-2995, https://doi.org/10.1007/s10489-017-1128-4.
10. Aydemir G, Acar B. Anomaly monitoring improves remaining useful life estimation of industrial machinery. Journal of Manufacturing Systems 2020; 56: 463-469, https://doi.org/10.1016/j.jmsy.2020.06.014.
11. Sun HB, Cao DL, Zhao ZD, Kang X. A hybrid approach to cutting tool remaining useful life prediction based on the Wiener process. IEEE Transactions on Reliability 2019; 67(3): 1294-1303, https://doi.org/10.1109/TR.2018.2831256.
12. Wang FF, Tang SJ, Sun XY, Li L, Yu CQ, Si XS. Remaining useful life prediction based on nonlinear random coefficient regression model with fusing failure time data. Journal of Systems Engineering and Electronics 2023; 34(1): 247-258, https://doi.org/10.23919/JSEE.2023.000006.
13. Kang R, Gong WJ, Chen YX. Model-driven degradation modeling approaches: Investigation and review. Chinese Journal of Aeronautics 2020; 33(4): 1137-1153, https://doi.org/10.1016/j.cja.2019.12.006.
14. Yan T, Lei YG, Li NP, Wang B, Wang WT. Degradation modeling and remaining useful life prediction for dependent competing failure processes. Reliability Engineering and System Safety 2021; 212: 107638, https://doi.org/10.1016/j.ress.2021.107638.
15. Cannarile F, Baraldi P and Zio E. An evidential similarity-based regression method for the prediction of equipment remaining useful life

in presence of incomplete degradation trajectories - Science Direct. Fuzzy Sets and Systems 2019; 367(15): 36-50, https://doi.org/10.1016/j.fss.2018.10.008.
16. Hassler U. Stochastic processes and calculus. Switzerland: SpringerLink 2016; 151-177. https://doi.org/10.1007/978-3-319-23428-1_7
17. Cao XR, Peng KX. Stochastic Uncertain Degradation Modeling and remaining useful life prediction considering aleatory and epistemic uncertainty. IEEE Transactions on Instrumentation and Measurement 2023; 72: 3505112, https://doi.org/10.1109/TIM.2023.3236323.
18. Yu WN, Tu WB, Kim IY, Mechefske C. A nonlinear-drift-driven Wiener process model for remaining useful life estimation considering three sources of variability. Reliability Engineering and System Safety 2021; 212: 107631, https://doi.org/10.1016/j.ress.2021.107631
19. Wu B, Zeng JC, Shi H, Zhang XH, Shi GN, Qin YK. Multi-sensor information fusion-based prediction of remaining useful life of nonlinear Wiener process. Measurement Science and Technology 2022; 33: 105106, https://doi.org/10.1088/1361-6501/ac7636.
20. Guan QL, Zuo ZY, Teng YQ, Zhang HX, Jia LM. Two-stage remaining useful life prediction based on the Wiener Process with multi-feature fusion and stage division. Eksploatacja i Niezawodność - Maintenance and Reliability. 2024; 26(4): 189803. https://doi:10.17531/ein/189803.
21. Wang ZQ, Hu CH, Fan HD. Real-time remaining useful life prediction for a nonlinear degrading system in service: application to bearing data. IEEE/ASME Transactions on Mechatronics 2018; 23: 211-222, https://doi.org/10.1109/TMECH.2017.2666199.
22. Zhang SY, Zhai QQ, Shi X, Liu XJ. A wiener process model with dynamic covariate for degradation modeling and remaining useful life prediction. IEEE Transactions on Reliability 2023; 72(1): 214-223, https://doi.org/10.1109/TR.2022.3159273.
23. Wu FH, Tang J, Jiang ZP, Sun YB, Chen Z, Guo BS.The remaining useful life prediction method of a hydraulic pump under unknown degradation model with limited Data. Sensors 2023, 23: 5931. https://doi.org/10.3390/s23135931
24. Kang JX, Lua YJ, Zhao B, Luo HB, Meng JC, Zhang YF. Remaining useful life prediction of cylinder liner based on nonlinear degradation model. Eksploatacja i Niezawodnosc - Maintenance and Reliability 2022; 24 (1): 62-69, http://doi.org/10.17531/ein.2022.2.8.
25. Hu CH, Pei H, Wang ZQ, Si XS, Zhang ZX. A new remaining useful life estimation method for equipment subjected to intervention of imperfect maintenance activities, Chinese Journal of Aeronautics 2018; 31(3): 514-528, https://doi.org/10.1016/j.cja.2018.01.009
26. Li NP, Lei YG, Guo L, Yan T, Lin J. Remaining useful life prediction based on a general expression of stochastic process models. IEEE Transactions on Industrial Electronics 2017; 64(7): 5709-5718, https://doi.org/10.1109/TIE.2017.2677334.
27. Mitici M, Pater ID. Online model-based remaining-useful-life prognostics for aircraft cooling units using time-warping degradation clustering. Aerospace 2021; 8(6): 168, https://doi.org/10.3390/aerospace8060168
28. Giorgio M, Mele A, Pulcini G. A perturbed gamma degradation process with degradation dependent non‐Gaussian measurement errors. Applied Stochastic Models in Business and Industry 2018; 158383682, https://doi.org/10.1002/asmb.2377
29. Liu Z. Generalized moment estimation for uncertain differential equations. Applied Mathematics and Computation 2021; 392: 125724, https://doi.org/10.1016/j.amc.2020.125724
30. Liu Y, Liu BD. Estimating unknown parameters in uncertain differential equation by maximum likelihood estimation. Soft computing 2022; 26: 2773-2780, https://doi.org/10.1007/s00500-022-06766-w.
31. Wang H, Liao HT, Ma XB. Remaining useful life prediction considering joint dependency of degradation Rrate and variation on time-varying operating conditions. IEEE Transactions on Reliability 2021; 70(2): 761-774, https://doi.org/10.1109/TR.2020.3002262.
32. Gribok A, Agarwal V, Yadav V. Performance of empirical Bayes estimation techniques used in probabilistic risk assessment. Reliability Engineering and System Safety 2020; 201: 106805, https://doi.org/10.1016/j.ress.2020.106805
33. Du YP, Katib I. Parameter estimation of nonlinear output error system under variational Bayesian method based on probabilistic graphical model. Fractals 2022; 30(2): 2240075, https://doi.org/10.1142/S0218348X22400758
34. Kumar A, Ghosh AK. Regularization regression methods for aerodynamic parameter estimation from flight data. Aircraft Engineering and Aerospace Technology 2023; 95(5): 820-830, https://doi.org/10.1108/AEAT-09-2019-0179.
35. Xie LY, Wu NX, Yang XY. A minimum discrepancy method for Weibull distribution parameter estimation. International Journal of Structural Stability and Dynamics. 2023; 23(8): 2350085, https://doi.org/10.1142/S0219455423500852.
36. Noorani I, Mehrdoust F. Parameter estimation of uncertain differential equation by implementing an optimized artificial neural network. Chaos,Solitons and Fractals 2022; 165: 112769, https://doi.org/10.1016/j.chaos.2022.112769
37. Jiang NT, Zhang N. Expectation maximization-based target localization from range measurements in multiplicative noise environments.

IEEE Communications Letters 2021; 25(5): 1524-1528, https://doi.org/10.1109/LCOMM.2021.3050455.

38. Chen J, Mao YW, Hu MF, Guo LX, Zhu QM. Decomposition optimization method for switching models using EM algorithm. Academic Journal 2023; 111(10): 9361-9375, https://doi.org/10.1007/s11071-023-08302-3.
39. Wang X. Wiener processes with random effects for degradation data, Journal of Multivariate Analysis, 2010; 101(2): 340-351, https://doi.org/10.1016/j.jmva.2008.12.007.
40. Si XS, Wang WB, Hu CH, Zhou DH, Pecht MG. Remaining useful life estimation based on a nonlinear diffusion degradation process. IEEE Transactions on Reliability 2012; 61(1): 50-67, https://doi.org/10.1109/TR.2011.2182221.
41. Zheng JF, Hu CH, Si XS, Zhang ZX, Zhang X. Remaining useful life estimation for nonlinear stochastic degrading systems with uncertain measurement and unit-to-unit variability. Acta Automatica Sinica 2017; 43(2): 259-270, https://doi.org/10.16383/j.aas.2017.c150775.
42. Lei YG, Han TY, Wang B, Li NP, Yan T, Yang J. XJTU-SY rolling element bearing accelerated life test datasets: a tutorial. Journal of Mechanical Engineering 2019; 55(16):1-6, https://doi.org/10.3901/JME.2019.16.001.
43. Wikipedia F. Spearman rank correlation coefficient. Switzerland: SpringerLink 2013; 23-28.